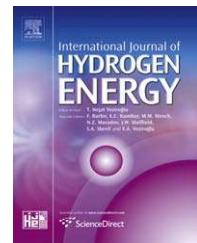




Available at www.sciencedirect.com



journal homepage: www.elsevier.com/locate/he



Recent Canadian advances in nuclear-based hydrogen production and the thermochemical Cu–Cl cycle

G. Naterer^{a,*}, S. Suppiah^b, M. Lewis^c, K. Gabriel^d, I. Dincer^e, M.A. Rosen^e, M. Fowler^f, G. Rizvi^g, E.B. Easton^h, B.M. Ikedaⁱ, M.H. Kaye^j, L. Lu^j, I. Pioroⁱ, P. Spekkens^k, P. Tremaine^l, J. Mostaghimi^m, J. Ausecⁿ, J. Jiang^o

^aCanada Research Chair Professor, University of Ontario Institute of Technology (UOIT), 2000 Simcoe Street, Oshawa, Ontario L1H 7K4, Canada

^bManager, Hydrogen Isotopes Technology Branch, AECL, Chalk River, Ontario K0J 1J0, Canada

^cChemist, Chemical Engineering Division, Argonne National Laboratory, 9700 S. Cass Avenue, Argonne, Illinois 60439, USA

^dAssociate Provost, Research, UOIT, 2000 Simcoe Street North, Oshawa, Ontario L1H 7K4, Canada

^eProfessor of Mechanical Engineering, UOIT, 2000 Simcoe Street North, Oshawa, Ontario L1H 7K4, Canada

^fAssistant Professor of Chemical Engineering, University of Waterloo, 200 University Avenue, Waterloo, Ontario N2L 3G1, Canada

^gAssistant Professor of Mechanical Engineering, UOIT, 2000 Simcoe Street North, Oshawa, Ontario L1H 7K4, Canada

^hAssistant Professor of Chemistry, UOIT, 2000 Simcoe Street North, Oshawa, Ontario L1H 7K4, Canada

ⁱAssociate Professor, Faculty of Energy Systems and Nuclear Science, UOIT, 2000 Simcoe St., Oshawa, ON L1H 7K4, Canada

^jAssistant Professor, Faculty of Energy Systems and Nuclear Science, UOIT, 2000 Simcoe Street, Oshawa, Ontario L1H 7K4, Canada

^kVice President of Science and Technology Development, Ontario Power Generation, 889 Brock Road, Pickering, Ontario, Canada

^lProfessor of Chemistry, University of Guelph, 50 Stone Road East, Guelph, Ontario N1G 2W1, Canada

^mCanada Research Chair Professor, Mechanical Engineering, University of Toronto, Toronto, Ontario M5S 3E5, Canada

ⁿAssistant Professor, Faculty of Energy Technology, University of Maribor, Hocevarjev trg 1, 8270 Krsko, Slovenia

^oProfessor and NSERC/UNENE Senior Industrial Research Chair, Electrical and Computer Engineering, University of Western Ontario, London, Ontario N6A 5B9, Canada

ARTICLE INFO

Article history:

Received 12 December 2008

Received in revised form

27 January 2009

Accepted 27 January 2009

Available online 27 February 2009

Keywords:

Nuclear-based hydrogen production

Thermochemical copper-chlorine

cycle

Electrolysis

ABSTRACT

This paper presents recent Canadian advances in nuclear-based production of hydrogen by electrolysis and the thermochemical copper-chlorine (Cu–Cl) cycle. This includes individual process and reactor developments within the Cu–Cl cycle, thermochemical properties, advanced materials, controls, safety, reliability, economic analysis of electrolysis at off-peak hours, and integrating hydrogen plants with Canada's nuclear power plants. These enabling technologies are being developed by a Canadian consortium, as part of the Generation IV International Forum (GIF) for hydrogen production from the next generation of nuclear reactors.

© 2009 International Association for Hydrogen Energy. Published by Elsevier Ltd. All rights reserved.

* Corresponding author.

E-mail address: greg.naterer@uoit.ca (G. Naterer).

1. Introduction

The threat of climate change has been well recognized. It is widely accepted that greenhouse gas emissions from fossil fuels are contributing to global warming and climate change. In contrast, hydrogen is a clean energy carrier. But hydrogen is a paradoxical – clean to use, but most current production processes for hydrogen also generate carbon dioxide. Most of the world's hydrogen (about 97%) is currently derived from fossil fuels through some type of reforming process. Thus, a key future challenge will be sustainable large-scale production of hydrogen at low cost. This paper presents the latest Canadian research in sustainable hydrogen production from nuclear energy, for a carbon free source of hydrogen.

Large quantities of hydrogen are needed by many industrial sectors, such as the Canadian oil sands (bitumen upgrading), agricultural (ammonia for fertilizers) and petroleum product industries. In the transportation sector, it is widely believed that hydrogen will eventually become a dominant energy carrier. The concept of a 'Hydrogen Economy' refers to hydrogen used as an energy carrier. Hydrogen is a desirable energy vector because it can be stored and used to generate electricity, either onboard vehicles or stationary power systems [1]. Hydrogen as a transportation fuel has a promising potential to significantly reduce urban pollution and greenhouse gas emissions. Recently there has been growing interest in hybrid and electric vehicles. But electricity storage issues (for example, a short range of electric vehicles compared to hydrogen fueled vehicles, due to the low energy density of batteries) limit the use of electricity as an energy carrier. Also, battery recharge times, cold weather performance, and durability will have to significantly improve before purely electric vehicles can become widely adopted in the transportation sector. Even with the potential emergence of electric vehicles, hydrogen will still be required as a 'range extender' fuel in hybrid vehicles. The envisioned hydrogen economy would require significant increases to the current power generation capacity to support all light duty vehicles. Thus, efficient large-scale production of hydrogen will be required in the future.

Thermochemical water splitting is a promising technology for large-scale sustainable production of hydrogen. Using intermediate compounds, a sequence of chemical and physical processes decompose water into hydrogen and oxygen, without releasing any pollutants externally to the atmosphere. The intermediate compounds are re-cycled internally within a closed loop. Over 200 thermochemical cycles have been identified previously [2,3]. But very few have progressed beyond theoretical calculations to working experimental demonstrations that establish scientific and practical feasibility of the thermochemical processes.

The sulfur-iodine (S-I) cycle is a leading example where equipment has been scaled up to a pilot plant level. Active development is underway at General Atomics (USA), Sandia National Laboratory (USA), Japan Atomic Energy Agency (JAEA), CEA (France) and others [4,5]. Approximately 30 l/h of hydrogen were produced from an S-I pilot facility by JAEA [4]. It aims to scale up the S-I cycle to much larger production capacities that could eventually support a significant volume of fuel cell vehicles. Korea (KAERI), China and Canada [6] are also

advancing towards large-scale production of hydrogen from nuclear energy. This paper provides an overview of Canada's latest advances in thermochemical hydrogen production, with particular focus on the copper-chlorine (Cu-Cl) cycle.

After considering factors of availability and abundance of materials, simplicity, chemical viability, thermodynamic feasibility and control/safety issues, the following seven cycles (in addition to the S-I cycle) were identified in a Nuclear Hydrogen Initiative [3] as the most promising cycles: copper-chlorine (Cu-Cl) [7], cerium-chlorine (Ce-Cl) [8], iron-chlorine (Fe-Cl) [8], vanadium-chlorine (V-Cl) [8], copper-sulfate (Cu-SO₄) [8] and hybrid chlorine [8]. Proof-of-principle demonstrations have been completed for these cycles and chemical viability has been proven. However, most of these cycles require process heat over 800 °C from very high temperature Generation IV reactor capabilities, which are not available with current nuclear technology and entail major design and material challenges. Due to lower temperature requirements around 550 °C and lower, the Cu-Cl cycle is a promising alternative that could be eventually linked with the Generation IV SCWR (Super-Critical Water Cooled Reactor) or ultra-super-critical thermal stations.

The Cu-Cl cycle has numerous advantages over other existing methods of hydrogen production, specifically lower environmental impact than carbon-based technologies. In comparison to conventional electrolysis, it has a significant margin of superior overall conversion efficiency, with more than one-third improvement over electrolysis. This excludes even larger gains if "waste heat" is utilized in the thermochemical cycle. It has much lower operating temperatures than other thermochemical cycles, thereby potentially reducing material and maintenance costs. Also, it can effectively utilize low-grade waste heat, thereby improving cycle and power plant efficiencies. Other advantages include lower demands on materials of construction, common chemical agents and reactions going to completion without side reactions.

Current collaboration between UOIT, AECL, Argonne National Laboratory and partner institutions, is focusing on enabling technologies for the Cu-Cl cycle, through the Generation IV International Forum (GIF; [7]). This paper focuses on recent Canadian developments to scale up these enabling technologies to larger capacities of hydrogen production with the Cu-Cl cycle, as well as synergies with electrolysis during off-peak hours when electricity demand and prices are lowest. Thermal efficiency and individual process developments within the Cu-Cl cycle will be presented, as well as corrosion resistant materials, controls/safety, reliability and linkage between nuclear and hydrogen plants.

2. Thermochemical copper-chlorine (Cu-Cl) cycle

2.1. Overview of the Cu-Cl cycle

The Cu-Cl cycle uses a set of reactions to achieve the overall splitting of water into hydrogen and oxygen as follows: H₂O (g) → H₂ (g) + 1/2O₂ (g). The Cu-Cl cycle decomposes water into hydrogen and oxygen through intermediate copper and

chloride compounds. These chemical reactions form a closed internal loop that re-cycles all chemicals on a continuous basis, without emitting any greenhouse gases. Process steps in the Cu–Cl cycle and a schematic realization of the cycle are shown in Table 1 and Fig. 1, respectively.

Two different variations of the Cu–Cl cycle are currently under investigation: 5-step and 4-step cycles. In the former case (5-step cycle), aqueous cupric chloride is first dried into a solid product of cupric chloride particles; then fed to the hydrolysis reactor to produce copper oxychloride. The latter case (4-step cycle) combines these processes together by supplying aqueous cupric chloride into the hydrolysis chamber, such as spraying the solution with co-flowing steam to produce the same copper oxychloride product. The 4-step process has an advantage of reducing complexity by eliminating the solids handling and thus less equipment. However, the 5-step process may be advantageous from the viewpoint of energy and exergy efficiencies, because lower grade heat can be used to remove the water in the drying process, rather than high temperature heat in the hydrolysis reactor for the unnecessary latent heat of vaporization of water.

Thermochemical hydrogen production with the Cu–Cl cycle is much more efficient than electrolysis via thermal power plants, because heat is used directly to produce hydrogen, rather than indirectly to first produce electricity, after which hydrogen is generated. A 42% efficiency (electricity) with the Generation IV reactor (SCWR; Super-Critical Water Reactor) leads to about 30% net efficiency by electrolysis for hydrogen production. In contrast, a 54% heat-to-hydrogen efficiency has been demonstrated from Aspen Plus simulations for the Cu–Cl cycle [9], although 43% is more realistic. This is a significant margin of superior overall conversion efficiency, with more than one-third improvement over electrolysis, excluding much larger gains if “waste heat” is utilized in the Cu–Cl cycle.

2.2. Thermochemical process for hydrogen production

Step 1 in the Cu–Cl cycle is the H₂ production step, which occurs at 430–475 °C, characterized by the reaction 2Cu(s) + 2HCl(g) → H₂(g) + 2CuCl(l) (see Table 1). Copper particles enter the reactor vessel and react with HCl gas to generate H₂

gas and molten CuCl. Scientific feasibility of this chemical reaction has been demonstrated experimentally by Serban et al. [10]. The conversion of HCl to hydrogen was found to be a function of Cu particle size as shown in Fig. 2 [10]. The yields varied between 65 and 100%, with complete conversion in the case of 3-μm Cu particles. The 100-μm Cu particles were obtained in an electrolytic cell by disproportionating CuCl to Cu and CuCl₂. The size and shape of electrolytic copper particles were affected by the operating parameters of the cell. To directly measure the kinetics of the reaction between HCl and Cu, the reaction rates were measured at four different temperatures (400, 425, 450 and 475 °C). The molar ratio of HCl in Ar was varied between 0.33 and 0.67.

The hydrogen yields were determined by comparing the measured amount of hydrogen produced vs. the stoichiometric amount of hydrogen that would be formed if all of the Cu was oxidized to CuCl. Hydrogen yields decreased with larger Cu particle size, indicating that high surface areas of contact between HCl and Cu are necessary for high hydrogen yields. Fig. 2 shows SEM (scanning electron microscope) images of the spheroidal and dendritic Cu particles used in the hydrogen generation reaction. No gaseous products other than hydrogen and HCl were observed in the effluent stream. X-ray diffraction (XRD) examination of the solid product resulting from the reaction showed patterns only for CuCl and Cu. No secondary reactions were favoured in the temperature range studied. Current experimental work is scaling up the process to generate larger capacities of hydrogen production (about 3 kg/day in a much larger reactor).

2.3. Electrochemical process of hydrogen production (4-step Cu–Cl cycle)

An electrochemical process is required, either separately from the hydrogen reaction (separate steps 1 and 2 in Table 1), or combining electrochemical and thermochemical processes together to produce hydrogen directly via electrolysis. This section discusses the latter process of cuprous chloride/HCl electrolysis. Oxidation of cuprous chloride (CuCl) during an electrochemical reaction occurs in the presence of hydrochloric acid (HCl) to generate hydrogen. The cuprous ion is

Table 1 – Steps and chemical reactions in the Cu–Cl cycle

Step	Reaction	Temp. Range (°C)	Feed/output ^a
1	2Cu(s) + 2HCl(g) → 2CuCl(l) + H ₂ (g)	430–475	Feed: Electrolytic Cu + dry HCl + Q Output: H ₂ + CuCl(l) salt
2	2CuCl(s) → 2CuCl(aq) → CuCl ₂ (aq) + Cu(s)	Ambient (electrolysis)	Feed: Powder/granular CuCl and HCl + V Output: Electrolytic Cu and slurry containing HCl and CuCl ₂
3	CuCl ₂ (aq) → CuCl ₂ (s)	<100	Feed: Slurry containing HCl and CuCl ₂ + Q Output: Granular CuCl ₂ + H ₂ O/HCl vapours
4	2CuCl ₂ (s) + H ₂ O(g) → CuO*CuCl ₂ (s) + 2HCl(g)	400	Feed: Powder/granular CuCl ₂ + H ₂ O(g) + Q Output: Powder/granular CuO*CuCl ₂ + 2HCl(g)
5	CuO*CuCl ₂ (s) → 2CuCl(l) + 1/2O ₂ (g)	500	Feed: Powder/granular CuO*CuCl ₂ (s) + Q Output: Molten CuCl salt + oxygen

Note: alternative 4-step cycle combines above steps 1 and 2 to produce hydrogen directly as follows: 2CuCl(aq) + 2HCl(aq) → H₂(g) + 2CuCl₂(aq) (Fig. 1 illustrates this 4-step version of the Cu–Cl cycle).

a Q = thermal energy, V = electrical energy.

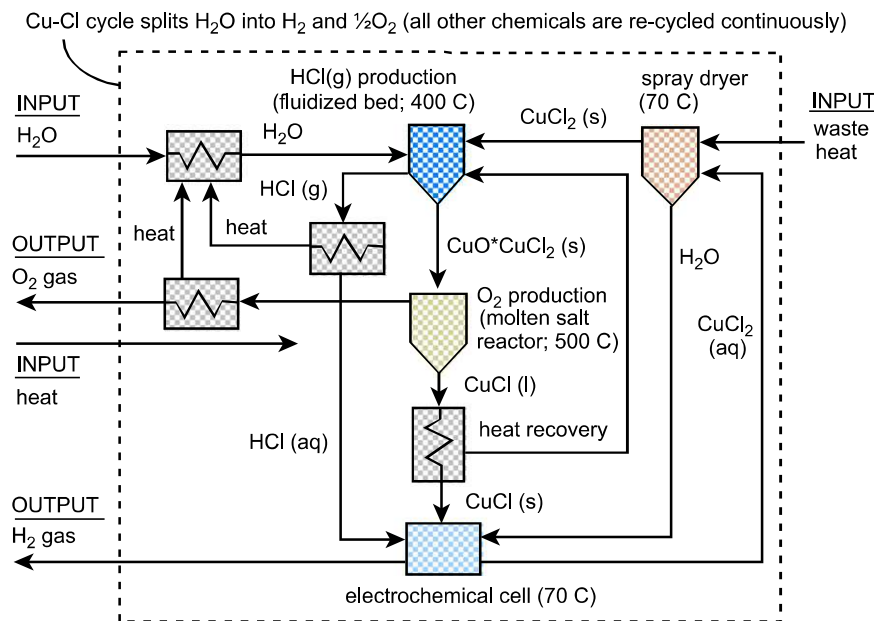


Fig. 1 – Schematic of the copper-chlorine (Cu-Cl) cycle.

oxidized to cupric chloride at the anode, and the hydrogen ion is reduced at the cathode (see Fig. 3).

AECL has demonstrated experimentally a CuCl electrolyzer in which hydrogen is produced electrolytically at the cathode and Cu(I) is oxidized to Cu(II) at the anode. A schematic of the experimental layout is illustrated in Fig. 4. AECL has conducted both half-cell and single cell reactions. The cathodic half reaction is given by the following equation,



where 6 M HCl was used in the experiments. This prevents the precipitation of CuCl (s) that forms when the chloride ion concentration is less than 1 M. When the chloride ion concentration is greater than 1 M, several anionic Cu(I) species can form [10]. Thus, several reactions are possible for the anodic half-cell:

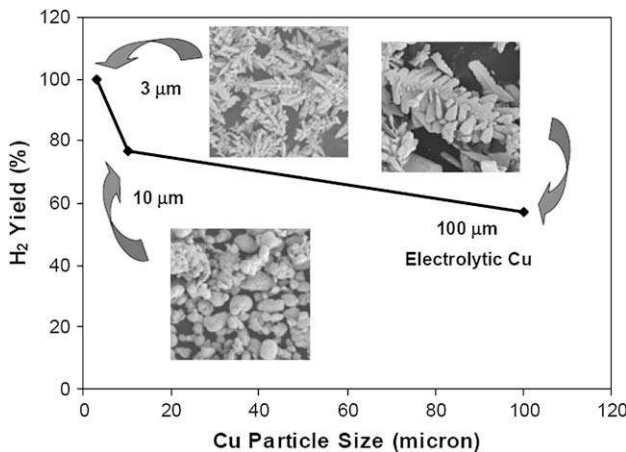
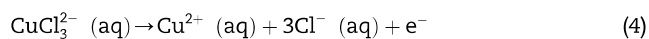
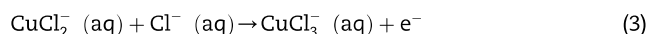
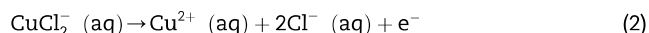
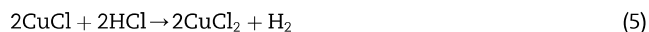


Fig. 2 – Hydrogen yields in a fixed bed reactor [11]; temperature = 450 °C, HCl flow rate = 2.5 cm³/min, 0.5 g of commercial (3 and 10 μm particle sizes) and electrolytic Cu (100 μm particle size).



The anodic reactions have been found to require no noble metal catalyst. It proceeds readily on graphite electrodes. However, the hydrogen production cathodic reaction requires a catalyst. Half-cell studies show that the rate of the CuCl/HCl electrolysis reaction increases with temperature and CuCl concentration. In the experiments, the solution concentration in the anode is 6 M HCl and about 1 M CuCl.

The overall cell reaction can be expressed as



A variety of electrode materials has been tested and hydrogen production was consistently observed at potentials as low as

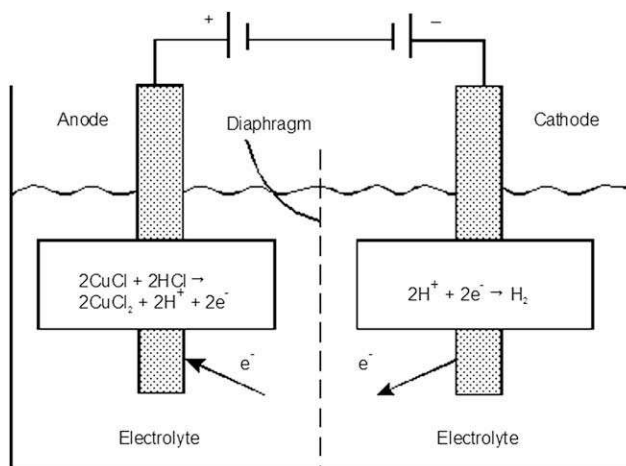


Fig. 3 – Schematic of the electrochemical cell.

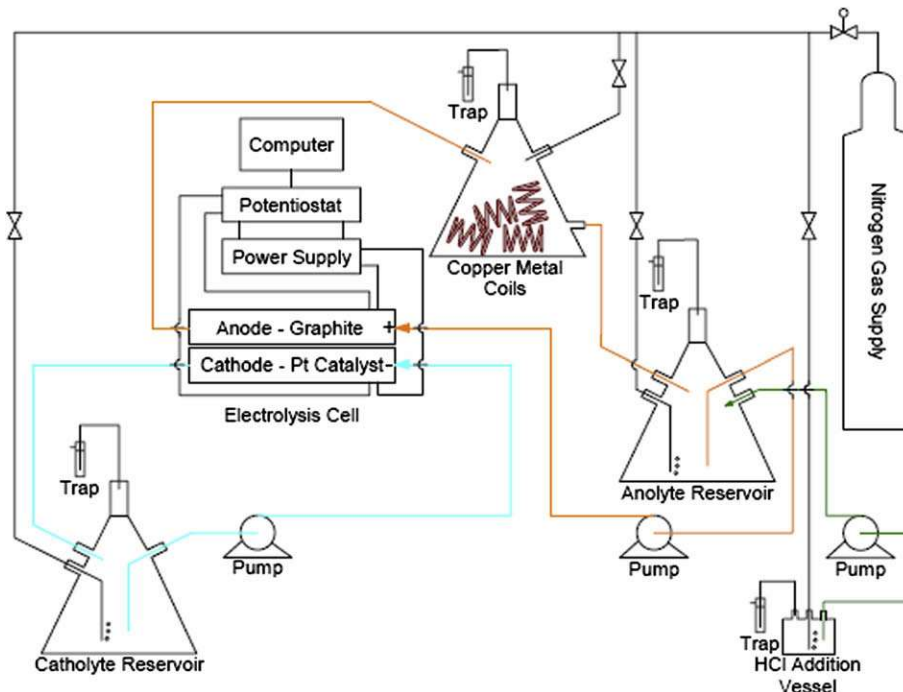


Fig. 4 – Experimental configuration of the electrochemical cell [11].

0.5 V. However, approximately 0.65 V was required to achieve good current density. Results have indicated that the reaction is feasible at reasonably low potentials and using relatively inexpensive electrode materials. Fig. 5 illustrates the effects of temperature on the current density vs. cell potential in a set of half-cell experiments. The current density is higher for a given cell emf at 80 °C than 25 °C.

A predictive formulation of the electrolysis process has been developed [11]. Comparisons were made between the predicted results and AECL's experimental data. The predicted activation potential showed reasonable agreement with measured data [11]. This difference occurred due to the measured uncertainty of the ROCV (reversible open circuit voltage), as well as copper ions or impurities present in the cell. The voltage loss in the electrolysis cell includes the surface overpotential, ohmic overpotential and concentration overpotential. The activation losses correspond to the voltage required in overcoming the open circuit voltage of the cell, when no load is connected in the circuit. Ohmic losses occur as a result of the internal resistance of the cell.

2.4. Electrochemical process of copper production (5-step Cu–Cl cycle)

A fundamental investigation of the anode electrode materials has been undertaken by Easton et al. [12] for the 5-step cycle (see Table 1). Their experiments employed three-electrode cell measurements using various working electrode materials. A 1 mM solution of CuCl (1 mM) in 1.5 M HCl, saturated calomel electrode (SCE) as the reference electrode, and Pt auxiliary electrode were used in all cases unless otherwise noted.

2.4.1. Carbon vs. Pt

The experiments focused on the influence of the electrode materials on the anode electrode kinetics. The primary goal was to determine if there is any performance gain by

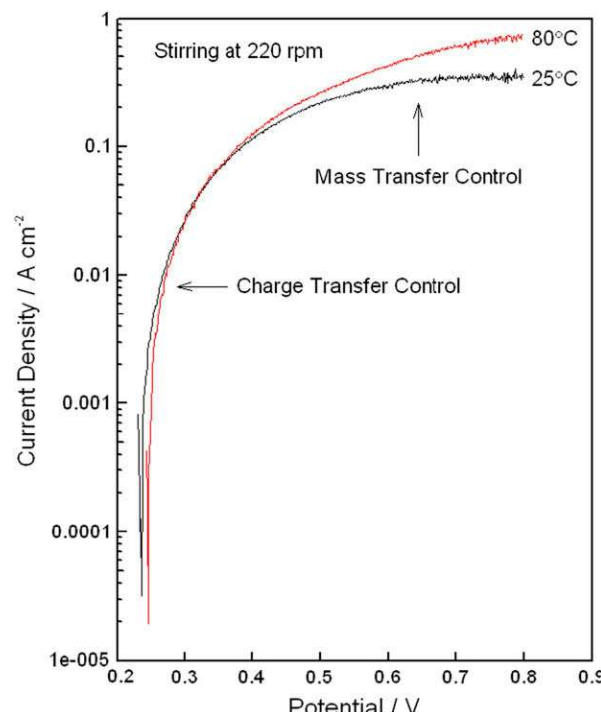


Fig. 5 – Current density vs. cell potential for two temperatures [11].

employing a noble metal based electrode material. Two materials were chosen: glassy carbon (GC) and Pt 5 mm diameter rotating disk electrodes (RDE). Cyclic voltammetry (CV) was performed with a stationary and rotating working electrode. No difference was observed in the potential requirements to drive the reaction on either a glassy carbon or Pt electrode surface. However, the limiting current densities with a Pt electrode surface were approximately three times larger than those achieved with a glassy carbon electrode.

Voltammetric measurements at different electrode rotation rates showed the typical Levich behaviour (limiting current proportional to square root of rotation rate) for both Pt and GC. However, the limiting currents were larger for Pt, indicating that there is a larger reaction rate on a Pt surface. Inverse Levich analysis allows for the determination of i_k , which represents the kinetic current density in the absence of mass transfer effects. From this analysis, i_k values were determined as $130 \mu\text{A cm}^{-2}$ and $40 \mu\text{A cm}^{-2}$ for Pt and GC, respectively.

These experiments suggested that better anode performance would be achieved if a Pt-based electrode material was employed on the anode due to its larger intrinsic specific activity. However, when one considers that a typical carbon supported Pt catalyst is 20 wt% Pt and 80 wt% carbon black, the performance gain by adding Pt is likely unnoticeable due to the much larger (about 14,000 times) carbon surface area. Thus, high surface area carbon blacks are the electrode materials of choice, based upon their performance and substantially lower cost.

2.4.2. pH dependence

In order for CuCl to remain in solution, the concentration of Cl^- must be maintained above 1 M. However, the source of Cl^- does not need to originate from HCl; it could originate from pH neutral salts such as NaCl [13]. There may be some benefit to the thermochemical cycle if less acidic conditions could be employed. A less corrosive environment may allow for lower cost materials to be used. However, the introduction of a salt like NaCl into the Cu-Cl cycle may complicate the extraction and separation of copper chloride compounds. In order to determine the impact of pH on the anode reaction, RDE measurements were performed as a function of pH. The level of pH was increased by dropwise addition of NaOH (aq) into the solution. Kinetic currents were determined as a function of pH. Measured results are shown in Fig. 6. When the pH is less than 2, i_k for Pt is approximately three times larger than the value for GC. Above a pH of 2, there is a significant increase in i_k for both electrodes. Furthermore, the difference between the i_k values for the GC and Pt electrodes becomes substantially smaller. For example, at a pH of 3.5, the values of i_k are $89 \mu\text{A cm}^{-2}$ and $109 \mu\text{A cm}^{-2}$ for GC and Pt, respectively. This further indicates that the kinetic advantage of Pt is even smaller at high pH.

2.4.3. Ceramic carbon electrodes

Another approach to increase the anode performance is to enhance both the surface area of the electrode and enhance the rate of diffusion of the Cu(I) species. Ceramic carbon electrodes (CCE) have been identified as a promising system for many electrochemical systems due to their high surface

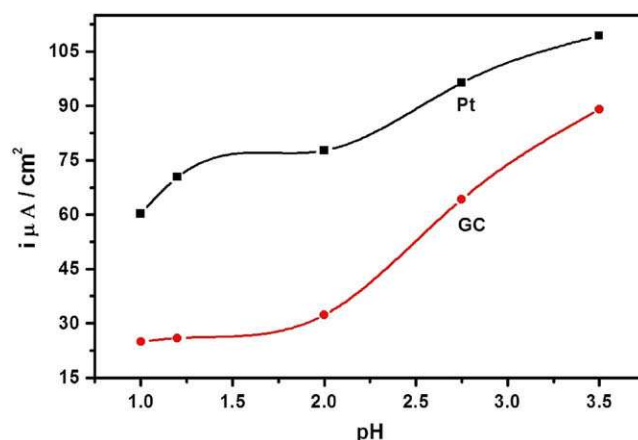


Fig. 6 – Kinetic current (i_k) for the $\text{Cu}^{+}/\text{Cu}^{2+}$ redox couple as a function of pH for glassy carbon (GC) and Pt electrodes (concentration of Cl^- was 1.5 M in all cases).

area and durability. CCEs consist of electronically conductive carbon particles that are bound together by a ceramic binder formed through the sol-gel process [14,15]. CCEs have found numerous electrochemical applications [16], including fuel cells. For example, Anderson et al. [17] have reported the use of CCE-based electrodes for direct methanol fuel cells.

Santhanam et al. [12] prepared CCE electrodes using an amino-functionalized silane precursor and Vulcan XC72 carbon black, which was applied onto the surface of carbon fiber paper (CFP). Under acidic conditions, the amino group was protonated, thereby making it an anion conductor, which will increase the diffusion of anionic Cu(I) species (e.g., CuCl_2) within the layer. Fig. 7 compares the CVs obtained with the CCE coated CFP electrode and a bare CFP electrode. It can be observed that a substantial enhancement (about 25-fold) of current is obtained when the CCE electrode was used.

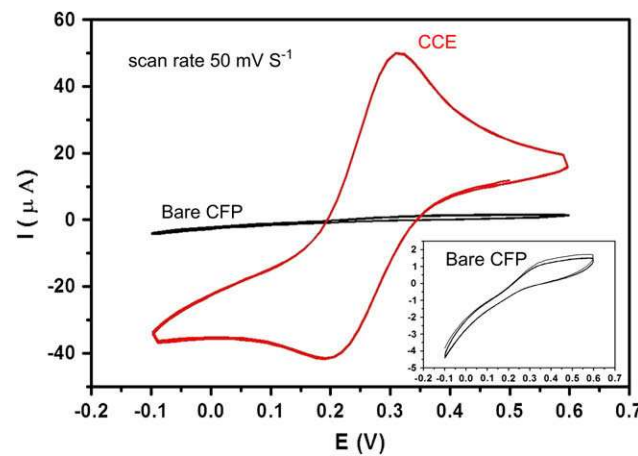


Fig. 7 – Cyclic voltammograms (CV) obtained for a CCE-based electrode and a bare carbon fiber paper (CFP) electrode (using 1 mM CuCl in the presence of 1.5 M HCl (aq)) [12].

2.5. Drying of aqueous cupric chloride

Step 3 of the Cu–Cl cycle is the drying step as expressed by: $2\text{CuCl}_2 \text{ (aq)} \rightarrow 2\text{CuCl}_2 \text{ (s)}$ (see Table 1). An aqueous CuCl_2 stream exiting from the electrochemical cell is supplied to a spray dryer to produce solid CuCl_2 (s), which is required for a subsequent hydrolysis step that produces copper oxychloride ($\text{CuO}^*\text{CuCl}_2$) and HCl gas. The apparatus must add sufficient heat to evaporate and remove the water. The process is an energy-intensive step within the Cu–Cl cycle. Although the amount of heat required for the drying step is much higher than other steps in the cycle, it occurs at a lower temperature (lower quality) and therefore with heat that is more readily available. Within the drying step, the energy requirement increases from 1 to 5 times higher for slurry feed to solution, respectively, depending on the CuCl_2 concentration. The overall cycle efficiency is higher with slurry feed in the drying step than drying of aqueous solution. The required heat can be obtained from low-grade waste heat to improve the cycle efficiency. Spray drying is an efficient method of water removal due to the relatively large surface area available for heat and mass transfer, provided the liquid atomizes into sufficiently small droplets (order of a hundred microns).

Experimental studies have been conducted to demonstrate the scientific feasibility of drying aqueous cupric chloride to produce solid CuCl_2 particles in a commercial spray dryer. Spray drying is a unique drying process that involves both particle formation and drying. The powder characteristics can be controlled and powder properties maintained constant throughout a continuous operation. Using a spray dryer, solid CuCl_2 particles have been successfully produced (see Fig. 8). The following spray dryer conditions were used in the

experiments: inlet air temperature = 200 °C, outlet air temperature = 112 °C, atomizing gas pressure = 2 bar, inlet gas pressure = 30 mbar, chamber pressure = 13 mbar, total mass of product = 183 g, density of product = 0.7 g/cm³.

Additional numerical studies [18] have been conducted to analyse the process of spray drying of aqueous cupric chloride droplets. The analysis assumed that evaporation results in a continuous shrinkage of the droplet with no solid core formation, but rather a continuous growth of CuCl_2 crystals, with the average thermal conductivity of the droplet remaining constant. Fig. 9 illustrates the variation of drying time with air velocity, temperature and operating pressure. It was observed that the drying time depends strongly on the inlet air humidity, temperature, particle size and operating pressure. At a low humidity of 0.0025 kg water/kg dry air, the drying time is less than 6 s for droplet sizes less than 200 μm, at 35 °C. At a humidity of 0.01 kg water/kg dry air, the drying time is less than 6 s for droplet sizes less than 100 μm, at 35 °C, and droplet sizes less than 150 μm, at 70 °C and 1 bar operating pressure. At low operating pressures of 0.5 bar, the drying time is less than 8 s for droplet sizes less than 200 μm, at 35 °C. The results predict that evaporative drying is possible down to temperatures as low as 35 °C, although such low temperature drying may limit the product quality and throughput.

2.6. Hydrolysis reaction for copper oxychloride production

The following hydrolysis reaction occurs within the Cu–Cl cycle (see Table 1): $\text{H}_2\text{O} \text{ (g)} + 2\text{CuCl}_2 \text{ (s)} \rightarrow \text{Cu}_2\text{OCl}_2 \text{ (s)} + 2\text{HCl} \text{ (g)}$. The reaction is an endothermic non-catalytic gas–solid reaction that operates between 350 and 400 °C. The solid feed to the hydrolysis reaction is cupric chloride, which comes from the dried CuCl_2 product of step 2 (electrolysis). Aqueous cupric chloride is dried to produce CuCl_2 solids, which are then transported to the hydrolysis chamber and reacted with superheated steam to produce copper oxychloride solid and hydrochloric gas. Recent developments have examined the transport phenomena

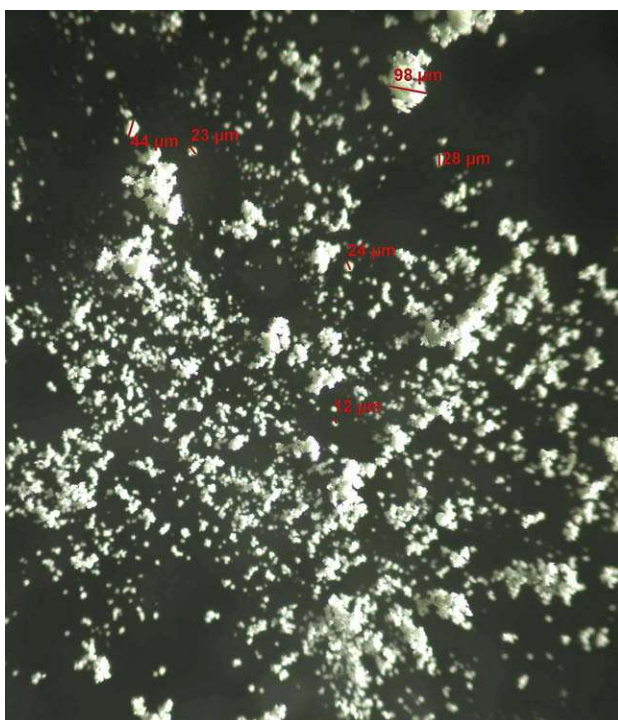


Fig. 8 – Cupric chloride particles produced from a spray dryer.

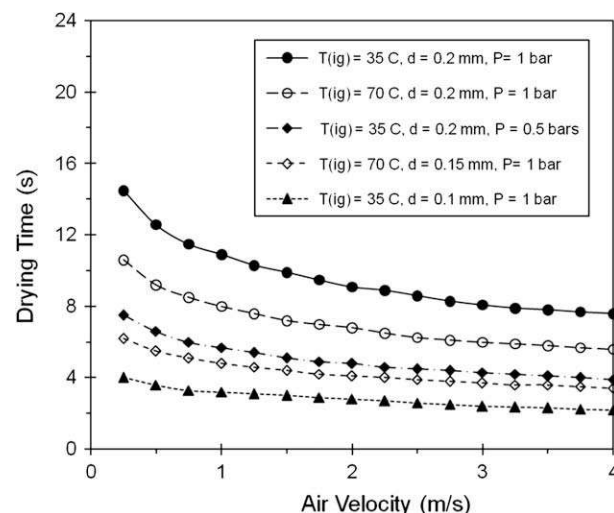


Fig. 9 – Predicted drying time at $H = 0.01 \text{ kg moisture/kg dry air}$ [12].

of reactive spray drying (a combination of the hydrolysis and drying processes), as well as a non-catalytic gas–solid reaction that separates drying and chemical reaction processes during hydrolysis.

Ferrandon et al. [20] have demonstrated experimentally the scientific practicality of the hydrolysis reaction to produce HCl gas and solid copper oxychloride. In order to vary the particle sizes, the material was first dried in a dessicator, crushed and sieved to the desired particle sizes and then rehydrated. During the hydrolysis experiments, the sample was heated rapidly (within 10 min) in humidified Ar to the reaction temperature, between 300 and 400 °C, and then held at the test temperature for a period, between 30 and 90 min.

The experimental conditions and the products analyzed are listed in Table 2. The first group of tests (Tests 1–3 in Table 2) was performed keeping the space velocity and steam/Cu molar ratio constant. The second group of tests (Tests 4–6 in Table 2) was performed keeping the space velocity and the H₂O vapor concentration constant. The test results were promising because they showed high yields of Cu₂OCl₂, up to 89 wt%. The steam to copper molar ratio in these tests varied from 28 to 66, while the CuCl content in the product varied from 8 to 12%. In order to minimize the decomposition reaction while keeping a low steam/Cu ratio, different operating parameters were varied (such as the test temperature, test duration, particle size of the starting CuCl₂ material, carrier gas flow rate and the steam concentration). In order to increase the gas velocity in the bed, the reactor tube diameter was reduced. The amount of CuCl significantly decreased when the reaction temperature was reduced. At 340 °C, the amount of CuCl in the sample was only 2.1 wt%. However, as the temperature decreased, less Cu₂OCl₂ was produced and more CuCl₂ remained unreacted.

The average conversion of solids depends on the rate of reaction and the residence time of a particle. A shrinking-core model has been developed to estimate the reaction rate of the gas–solid reaction [19]. If the diffusion of the gaseous reactant into a particle is much faster than the chemical reaction, the solid reactant is consumed nearly uniformly throughout the particle (see Fig. 10a). In this situation, a uniform-reaction model can be used. On the other hand, if the diffusion of gaseous reactant is much slower and it restricts the reaction zone to a thin layer that advances from the outer surface into the particle (Fig. 10b), then the shrinking-core model is adopted.

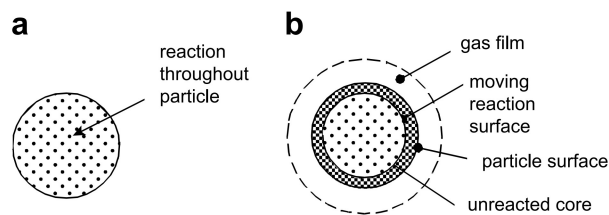


Fig. 10 – Schematic of (a) uniform conversion of the particle and (b) shrinking particle core.

The predicted variation of solid conversion time with vapor fraction in the gas is illustrated in Fig. 11. The experimental data in Ref. [20] was used for validation of the predicted solid conversion for uniformly sized particles of 200 μm diameter in plug flow of solids. As the mole fraction of steam in the gas increases, the time of solid conversion decreases. The reaction rate constant for the uniform-reaction model is $k_r = 0.00063 \text{ m}^3 (\text{STP})/\text{m}^2$ for solid conversion. At high conversions, all of the models predict essentially the same rate of conversion. The fraction of reacted core volume to the total particle volume increases over time, regardless of the resistance mode for mixed flow of solids.

2.7. Molten salt reactor for oxygen production

The oxygen production step (step 5; see Table 1) receives solid feed of CuO*CuCl₂ and produces O₂ gas and liquid cuprous chloride. The reaction is given by CuOCuCl₂ (s) = 2CuCl (molten) + 0.5O₂ (gas) at 530 °C. Gas species leaving the oxygen reactor include oxygen gas and potentially impurities of products from side reactions, such as CuCl vapor, chlorine gas, HCl gas (trace amount) and H₂O vapor (trace amount). The substances exiting the reactor are molten CuCl, potentially solid CuCl₂ from the upstream reaction (CuCl₂ hydrolysis step), due to the incomplete decomposition of CuCl₂ at a temperature lower than 750 °C, as well as reactant particles entrained by the flow of molten CuCl. In the oxygen reactor, copper oxychloride particles decompose into molten salt and oxygen. The reactant particles absorb decomposition heat from the surrounding molten bath.

Serban et al. [10] have demonstrated experimentally the scientific practicality of the oxygen production reaction at a small test-tube scale. Recent efforts have focused on

Table 2 – Experimental conditions and elemental analyses of the products after the hydrolysis reaction [11]

Test #	Steam/Cu molar ratio	Ar (ml/min)	Time (min)	GHSC (h ⁻¹)	H ₂ O vapor (%)	CuCl ^a (wt%)	CuCl ₂ ^b (wt%)	Cu ₂ OCl ₂ ^c (wt%)
1	28.3	200	60	43,327	8	12.1	1.0	86.9
2	27	195	43	43,313	10	15.5	1.3	83.2
3	27.1	185	28	43,079	14	14.8	5.2	80.0
4	38	160	20	43,135	26	16.4	10.8	72.8
5	52	160	30	43,135	26	8.0	3.2	88.8
6	66	160	40	43,135	26	11.1	1.5	87.4

^a Error: ±0.3.

^b Error: ±0.3–0.7.

^c Error: ±0.5–0.7.

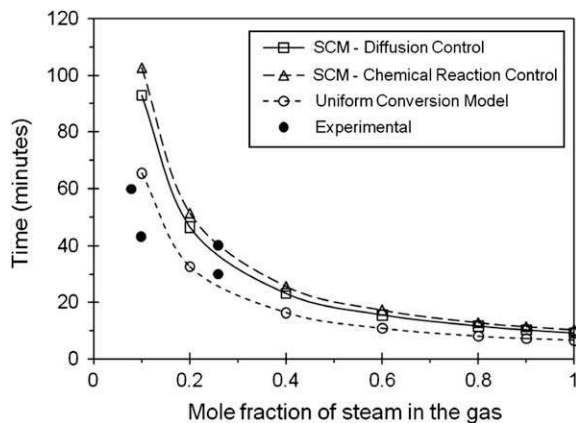


Fig. 11 – Comparison of solid conversion time with experimental data.

experimental work that scales up equipment beyond small test-tubes to much larger reactors. Several design issues must be addressed at these larger flow capacities [21,22]. For example, aggregation into blocks of $\text{CuO}^*\text{CuCl}_2$ particles may occur during the process of removing, conveying and feeding of particles. The aggregation may choke or clog the feeder and cause sudden spouting of particles.

Also, there may exist embedded particles of CuCl_2 from the upstream hydrolysis reactor. The existence of CuCl_2 particles in $\text{CuO}^*\text{CuCl}_2$ would lead to undesirable products and side reactions, i.e., CuCl_2 may decompose to CuCl and Cl_2 gas. If particles enter the reactor at a temperature lower than 430 °C, a difficulty with the presence of bubbles in the molten salt may occur. Some CuCl vapor might condense and molten CuCl might solidify around the $\text{CuO}^*\text{CuCl}_2$ particles. If an aggregation develops with particles, molten salt and bubbles, the contact area between a reactant particle and heating medium (molten CuCl) will decrease and the aggregations may float along the surface of the molten salt. This would deter the decomposition of reactant particles and potentially lead to choking of the reactor (a major safety concern). These design issues and others are currently under investigation for the large-scale experimental oxygen reactor.

3. Towards scale-up to a thermochemical pilot plant

In order to scale up the previous enabling technologies for hydrogen production with the Cu–Cl cycle, a number of future developments are needed in selected technologies that are critical to equipment scale-up. This section outlines these related advances in the overall analysis, thermochemistry and electrochemistry of working fluids, advanced materials, safety and eventual linkage with nuclear plants.

3.1. Thermal and life cycle analyses of the Cu–Cl cycle

Water is decomposed into hydrogen and oxygen as the net result of the Cu–Cl thermochemical cycle. The cycle involves five steps, as listed in Table 1: (1) HCl(g) production using

equipment such as a fluidized bed, (2) oxygen production, (3) copper (Cu) production, (4) drying, and (5) hydrogen production. In this section, the steps are assessed thermodynamically using energy and exergy methods that consider the relevant chemical reactions. For example, energy and exergy efficiencies of the hydrogen production step are evaluated and parametric studies are conducted for energetic and exergetic balances, considering variable reaction and reference-environment temperatures.

Recent studies by Chukwu et al. [23] and Orhan et al. [24] have analyzed the overall thermal efficiency of the 5-step Cu–Cl cycle. The efficiency of the cycle vs. temperature was analyzed for three cases: $x = 0.2, 0.3$, and 0.4 , where x refers to the fraction of heat loss to heat input in the cycle [24]. The calculated efficiencies varied from 42 to 55% at 550 °C. A life cycle analysis (LCA) was also conducted [12]. One objective of the LCA was to identify environmental issues associated with nuclear-produced hydrogen and determine which are the most critical. The study focused on identifying energy, materials, and waste in/out of the system for the nuclear–hydrogen plant. Sensitivity analyses were performed to investigate what future improvements should be made, and identify specific areas where significant contributions would improve the overall environmental impact.

Comprehensive energy and exergy analyses were performed with Aspen Plus and Engineering Equation Solver (EES) [23–29] to investigate the overall energy and exergy efficiencies of the entire cycle and its five primary steps for different cases, i.e., varying reaction temperatures, environment temperatures, pressures, chemical compositions, etc. The effects of heat losses were also studied. As an example, Fig. 12 shows the variation of energy (η_e) and exergy (η_{ex}) efficiencies of the Cu–Cl cycle with each step's range of temperatures.

The overall energy efficiency of the Cu–Cl cycle, η_e , can be defined as the fraction of energy content of hydrogen based on its lower heating value, to the amount supplied:

$$\eta_e = \frac{\overline{LHV}_{\text{H}_2}}{\overline{Q}_{\text{in}} + \overline{Q}_{\text{loss}}} \quad (6)$$

where $\overline{LHV}_{\text{H}_2}$ is the lower heating value per kmol of hydrogen and \overline{Q}_{in} is the total energy demand by the process to produce a unit quantity of hydrogen. This total energy demand of the Cu–Cl cycle is the summation of all reaction heat flows of the

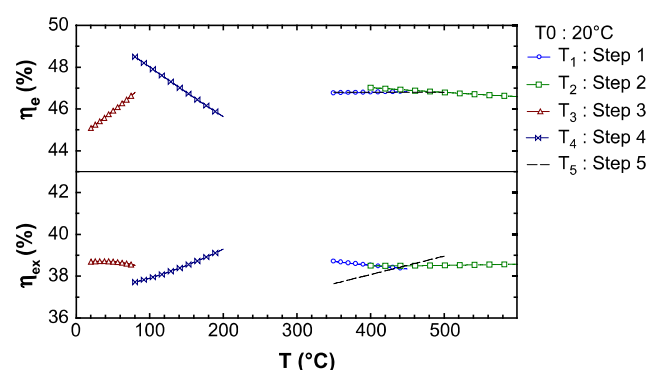


Fig. 12 – Process efficiencies over each temperature range (assumes 40% heat loss from cycle).

five main steps described previously. The lower heating value of hydrogen is 240,000 kJ/kmol H₂. Also, the exergy efficiency can be obtained using the following equation:

$$\eta_{ex} = 1 - \frac{\bar{e}\dot{X}_{destroyed}}{\bar{e}\dot{X}_{in}} \quad (7)$$

Sample results are presented in Fig. 12, based on an assumption that approximately 40% of the total energy supplied to the Cu–Cl cycle is lost through various internal processes. Given the current limitations of detailed operational data for an actual Cu–Cl plant, certain simplifying assumptions and approximations are needed, i.e., adiabatic vessels, reaction stoichiometry, materials of construction, by-products and side reactions, and so forth. Overall, it was assumed that the total heat loss (Q_{loss}) from the Cu–Cl cycle was a fixed percentage of the total heat supply (Q_{in}) into the cycle. In the analysis, when any process temperature was varied, others in other steps were kept constant.

A life cycle assessment (LCA) of the system is shown in Fig. 13. It illustrates the predicted environmental emissions and impacts, based on impact categories described in Ref. [24]. Brief explanations of the environmental impact categories and definitions are shown in Table 3. Emissions from the overall system are the sum of outputs from the nuclear power plant and thermochemical hydrogen plant. The relative contribution from each process in the life cycle of the hydrogen plant to the total environmental impact can be observed in Fig. 13. The results illustrate a typical trend, as various factors affect the results, such as the materials of construction, operating conditions and so forth.

From Fig. 13, construction of nuclear and thermochemical hydrogen plants will contribute to impact categories of EP, ODP and POCP (see Table 3 for definitions). The nuclear fuel cycle contributes to ADP and RAD. Operation of the nuclear plant does not contribute significantly to the total impact. The environmental impact for the operation of the thermochemical hydrogen plant contributes much less to the total emissions. Changes in the inventory of materials or chemicals needed by the thermochemical plant do not affect significantly the total environmental impact. The analysis uses various simplifying assumptions and approximations; for example, it does not consider the varying efficiencies of the thermochemical cycle at different conditions, fraction of product conversions, and so forth, which may lead to larger

Table 3 – Environmental impact categories and definitions

Environmental impact category	Definition
Abiotic resource depletion potential (ADP) (g extracted element)	Abiotic depletion involves the extraction of non-renewable raw materials
Global warming potential (GWP) (g CO ₂ -eq)	Amount of CO ₂ in the earth's atmosphere
Ozone depletion potential (ODP) (g CFC-eq)	Depletion of ozone layer leads to an increase in the ultraviolet radiation reaching the earth's surface
Eutrophication potential (EP) (kg phosphate-eq)	Over-fertilisation or nutrition enrichment at a certain location
Acidification potential (AP) (g SO ₂ -eq)	Acid depletion on soil and into water may lead to changes in the degree of acidity
Photochemical ozone creation potential (POCP) (kg ethene-eq)	Due to volatile organic compounds in the atmosphere
Radioactive radiation (RAD) (disability-adjusted life years, DALY)	Emission and propagation of energy in the form of rays or waves

raw material consumption. This research is still ongoing and it will improve the meaningfulness and accuracy of the results. Furthermore, a related improvement analysis will lead to reduced environmental impact of the combined nuclear and hydrogen plants. Further details of these life cycle studies are available in Ref. [24].

3.2. Thermochemical data for working fluids

Accurate self-consistent thermochemical data for the copper chlorides up to 200 °C are required, in order to improve solubility calculations and electrochemical modeling capabilities for Aspen Plus and OLI software. Experimental work has been initiated at the University of Guelph, Canada, and UOIT to determine a comprehensive thermochemical database, for solubility limits of OMIT, and aqueous cupric chloride vs. chloride concentration and temperature using UV-vis spectroscopy [12]. The chloride ion is obtained by adding LiCl OMIT. The conditions of tests are primarily 25–200 °C, up to 20 bar. Specialized equipment for this task is needed to reach elevated temperatures and pressures, because cupric chloride is chemically aggressive, and because changes in the solution concentrations must be made precisely. A titanium test cell has been custom made, including a UV-vis spectrometer with sapphire windows, HPLC pumps, and an automated injection system. The data acquired will be combined with past literature data for the cuprous chloride system to develop a self-consistent database for the copper(I) and copper(II) chloride–water systems.

Additional theoretical models have been developed at the University of Maribor, Slovenia, to determine thermodynamic properties of various Cu–Cl mixtures at elevated temperatures, including the specific heat, enthalpy and thermal conductivity [30]. Cupric chloride undergoes solid–solid and solid–liquid phase changes in the range of operating

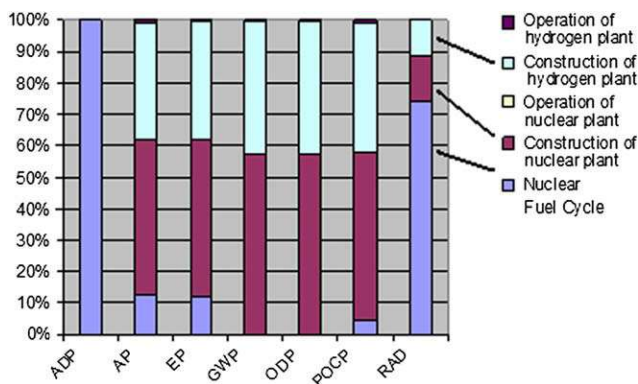


Fig. 13 – Contribution of different processes to the total environmental impact.

conditions of the thermochemical Cu–Cl cycle. Avsec and Naterer [30] examined the corresponding step changes of thermodynamic properties at phase transition. Analytical models were developed based on statistical thermodynamics and chain theory to improve thermophysical property predictions of CuCl and HCl in the liquid and gas regions [30].

3.3. Advanced membranes for the CuCl electrolysis process

Better performing electrode materials are needed for the electrochemical process in the Cu–Cl cycle. Additional collaboration between team members is underway for synthesis, conductivity measurements, and electrochemical performance testing of various membrane materials. This material testing involves primarily the electrolytes that conduct chloride ions, with both multi-nuclear spectroscopy and diffusion measurements. Targeted materials include organo-silica-based anion-selective membranes, as well as polymer-composites based on poly(benzimidazole). Studies of ion transport phenomena using solid-state NMR provide unique insight into the molecular-level processes.

Chloride transport within the membrane of the cell strongly affects performance of the electrochemical process. Studies of Cl[−] transport, however, are limited. Chlorine isotopes are not well understood NMR nuclei, due to the large quadrupole moments, and low resonance frequencies. However, the availability of ultra-high field NMR spectrometers, development of signal-enhancement techniques such as QCPMG, together with stepped-frequency approaches, have made the observation of quadrupolar nuclides such as chlorine more feasible. Collaboration with McMaster University, Canada, involves the characterization of anion-conducting membrane candidates using multi-nuclear MAS NMR spectroscopy. In addition, proton transport processes in electrolytes are conducted by applications of advanced multi-nuclear SSNMR methods. The application of homonuclear ¹H double quantum NMR spectroscopy for probing bonding structures, and site-specific assignment of relative dynamics, can reveal new insights into the structural vs. diffusion processes in candidate proton-conducting polymer electrolytes for the electrochemical process of the Cu–Cl cycle.

AECL research has shown that electrochemical generation of hydrogen at the cathode of the 4-step Cu–Cl cycle may be more promising than intermediate production of copper in the 5-step cycle. In the 4-step cycle, a cation exchange membrane that allows fast and efficient transport of protons would need to be employed in place of an anion exchange membrane. Polymer electrolyte membranes (PEM) that are commonly used in fuel cells and water electrolyzers such as Nafion™ could be employed. However, such a membrane will also be permeable to cationic copper species that could cross-over from the anode compartment into the cathode. Further studies of PEM materials in this type of cell are needed.

3.4. Safety and reliability

In collaboration between UOIT and the University of Western Ontario, Canada, reliability and probabilistic safety

assessments have been conducted for a nuclear-hydrogen plant using fault tree analysis (FTA) of potential risk scenarios. The risk levels of the thermochemical Cu–Cl plant under different accident scenarios were analyzed [31]. Based on the results, potential problems encountered in Cu–Cl cycle were identified and solutions recommended for future improvements.

Hydrogen is a flammable gas without odour and color. It burns with a nearly invisible flame, so monitoring leakages of H₂ is one of the safety challenges. If there is significant loss of integrity of the hydrogen storage and handling sub-system, the hydrogen generation reactor must stop operating, which would influence the operation of the whole system. Other potential accident scenarios related to the hydrogen generation process are overheating and over-pressurization of the reactor, since it is an exothermic reaction and accumulation of impurities will influence the release of heat inside. The use of hazardous chemicals in the process also presents risks to be managed. Fig. 14 shows a simplified sample fault tree for this process. HCl(g) mixes with particles of Cu to produce H₂. The flow of the HCl stream and size of Cu particles affect the fault tree analysis.

Since the fault tree construction is a top-down process, define the “H₂ formation reaction fails” as the top event in this fault tree. Two main scenarios could cause the top event to occur. These are the failure of the H₂ formation reactor, and generating other side products through incomplete reactions or improper conditions. In terms of the reaction requirements mentioned previously, the temperature and pressure of the reactor, and the leakage of hydrogen, are the sub-events if the reactor fails. Based on previous examples and practical experience, the lower levels of the fault tree can be built until the basic events are determined, when the reliability data can be obtained. In another branch, either improper reactants or passivation could cause the event of wrong products (side reactions) to occur. Similar fault trees and safety analyses have been reported for other parts of the Cu–Cl cycle [31]. Once the potential risks are identified, proper safety control systems have to be designed to mitigate those risks to an acceptable level. The safety control systems should be separate from the process control system, and they should satisfy desired safety grades and regulations.

3.5. Development of corrosion resistant materials

One of the challenging environments for materials to resist corrosion is the copper oxychloride decomposition reactor. In this reactor, a gaseous stream of pure oxygen is produced at temperatures between 450 and 550 °C. This stream may contain HCl or Cl₂ gas impurities and small quantities of entrained copper oxychloride. The impurity concentrations should be small because the hydrolysis reactor (feeding the decomposition reactor) will operate at negative pressures in order to enhance the performance of the hydrolysis reactor. High Ni–Cr alloys were identified as the most promising materials of construction for this environment because of their corrosion resistance in high temperature oxidizing environments.

The FACTSage thermochemical database was used to identify the thermodynamically stable phases that could exist

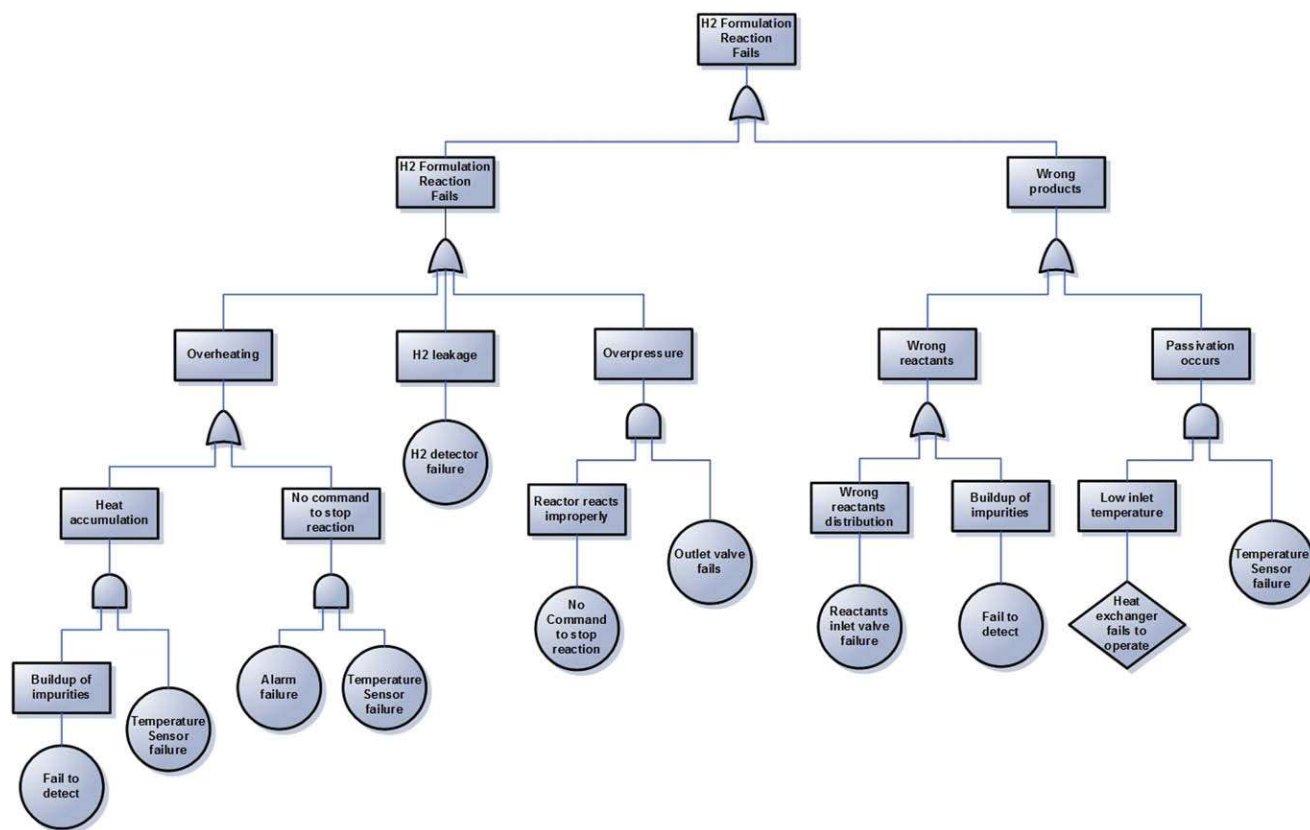


Fig. 14 – Fault tree of the hydrogen reactor [21].

in a system comprised of a pure metal, oxygen, HCl, and Cl₂ at 500 °C [12]. The predominant Fe, Ni, Cu, and Cr phases in an O₂/HCl/Cl₂ environment were determined. The equilibrium reaction boundary was plotted as a function of the partial pressures of O₂ and HCl, for a constant Cl₂ partial pressure. The resulting predominance diagrams were plotted over an O₂ and HCl partial pressure range of 10⁻²⁰–1 atm for Cl₂ partial pressures between 10⁻⁶ and 1 atm (see Fig. 15; [32]). The predominant Ni and Cr species are solids, suggesting that a corrosion resistant protective layer could be formed on the metal.

Further work is needed to demonstrate that these solids are the favoured corrosion products, and that they possess the appropriate properties for passivity and corrosion protection. In contrast, at very low O₂ partial pressures, the predominant Fe species is a gas. A small amount of O₂ will induce the formation of haematite (Fe₂O₃), indicating that Fe could form a protective layer during oxygen generation. It is common that the high-temperature iron oxides that are formed are less protective than the Cr or Mo oxides. The corrosion resistance of an alloy is the result of a compact inner layer containing Cr and/or Mo. The formation of a gaseous Fe corrosion product suggests that a low iron alloying content also would be desirable. This would avoid the creation of vacancies in the corrosion product layer, and avoid the formation of a potential contaminant in the product stream.

In Fig. 15, each line represents an equilibrium between the solid phases for a partial pressure of Cl₂: purple 10⁻⁶ atm, blue

10⁻⁴ atm, green 10⁻² atm, and red 1 atm (for interpretation of the references to colour in this figure, the reader is referred to the web version of this article). The NiCl₂ solid is stable below each horizontal line, while the NiO solid is stable above each horizontal line, and the Ni(OH)₂ solid is stable above each diagonal line. The solid lines represent equilibrium without constraining the total pressure of the system. The dotted lines represent the equilibrium state under a constraint of 1 atm total pressure for all gaseous species.

Advanced materials of construction are also needed for other reactors because of the high-temperature corrosive working fluids. Corrosion resistant coatings of amorphous metal alloys that can be deposited on complex shapes with large surface areas are being developed through collaboration between UOIT and the University of Toronto, Canada. The primary advantage of this type of coating is that the final structure is homogeneous and it contains few grain boundaries in the material, micro-segregation phases or dislocations.

Candidate materials and coating methods have been identified (see Table 4). Adding a ceramic layer on top of the amorphous metal layer could further improve the corrosion resistance of the material. Electrochemical testing of the coatings can be performed before and after exposure to the reactor environment. The overall integrity of the coating can be assessed using Linear Polarization methods. The effectiveness of the coating (porosity and thickness) can be measured using Electrochemical Impedance Spectroscopy

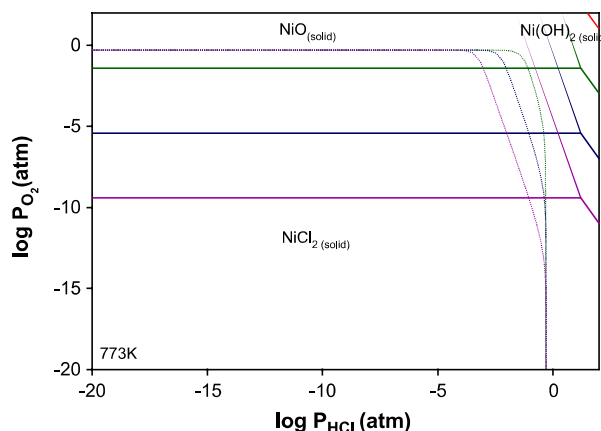


Fig. 15 – Predominance diagram for nickel in a chlorine/oxygen/HCl environment.

(EIS). The information about changes in coating porosity and thickness can be used to predict the lifetime of the coating.

3.6. Utilizing and upgrading waste heat

A unique advantage of the Cu–Cl cycle is an ability to utilize low-grade “waste heat” from power plants or other sources to aid hydrogen production, rather than rejecting that heat to the environment (such as a nearby lake). This could significantly improve the economics of hydrogen production, as well as potentially the generation of electricity. For example, a nuclear plant’s efficiency usually refers to electricity output alone, but the “efficiency” would be higher if nuclear energy contributed to production of another valuable energy carrier, hydrogen, from the same nuclear source. The Cu–Cl cycle’s efficiency implies that the heat supply comes at some “cost”. But if low-grade waste heat is utilized as a heat source at minimal or no cost, then the economics of hydrogen production is further improved and more attractive than other high-temperature thermochemical cycles that cannot use such low-grade heat.

Drying of aqueous cupric chloride (step 3; Table 1) is an energy-intensive process that requires heat at a relatively low

temperature, below 100 °C. Waste heat from the moderator vessel of CANDU nuclear reactors could be transferred by fluid through a pipeline over some distance to a nearby thermochemical hydrogen plant. Flow through a liquid–gas heat exchanger would then transfer this waste heat to a gas stream, which would be used as a drying medium in a spray dryer to produce CuCl₂ (s) in the Cu–Cl cycle [33]. Alternatively, heat pumps could upgrade the heat, either by chemical heat pumps that release heat at successively higher temperatures in exothermic reactors (i.e., salt/ammonia or MgO/vapor chemical heat pumps), or vapor compression heat pumps [34,35].

3.7. Linkage of nuclear and hydrogen plants

The Generation IV nuclear reactor, SCWR (Super-Critical Water Reactor) is being designed to operate at higher temperatures (550–625 °C) that can facilitate co-generation of electricity and hydrogen. SCWR is expected to co-generate electricity and hydrogen uniformly throughout the year, independently of the electrical load. With an electrical load decrease, the SCWR could produce more hydrogen and vice versa. Using high-temperature heat from a nuclear power plant to heat water in the hydrogen production loop is a promising option with SCWR. Heat exchangers of a recuperator-type would be used for this purpose (see Fig. 16). Currently, UOIT is collaborating with AECL on various plant configurations for co-generation of electricity and hydrogen [36].

4. Water electrolysis with off-peak electricity

Two technologies, applied in tandem, have a promising potential to generate hydrogen without leading to greenhouse gas emissions: (1) thermochemical Cu–Cl cycle and (2) electrolysis. This section focuses on recent advances in electrolysis from nuclear energy, including how it complements thermochemical production of hydrogen, when it becomes more economically advantageous and what benefits it can provide by storing hydrogen at off-peak hours when electricity prices are lowest.

Table 4 – Candidate materials for corrosion resistant coatings

Method of Spray	Materials	Advantages	Testing
HVAF	Ni–Nb–Ti–Zr–Co–Cu	High gas formation ability	1 M HCl potentiodynamic, potentiostatic, SEM, XRD, DSC, oxygen analyses
VPS	57Ni–20Zr–3Si–18Ti–2Sn	Crystallization reaction near 614 °C	1 M HCl potentiodynamic, potentiostatic, SEM, XRD, DSC, XPS, AES oxygen analyses
HVOF, VPS	Ni–Zr–Si–Ti–Sn	Higher glass formability, crystallization at 600 °C	SEM, XRD, DSC
HVOF Casting	Ni–Zr–Si–Ti–Sn Ni–Ta	Crystallization T = 770 °C, high corrosion resistance	SEM, XRD
HVOF	FeCrMoCBY	Crystallization T = 610 °C, high corrosion resistance	SEM, XRD, DSC, microhardness, wear, 1 M HCl potentiodynamic
Casting	Ni ₅₇ Nb ₃₃ Zr ₅ Co ₅	Crystallization T = 640 °C, high corrosion resistance	SEM, XRD, DSC, 6 M HCl potentiodynamic

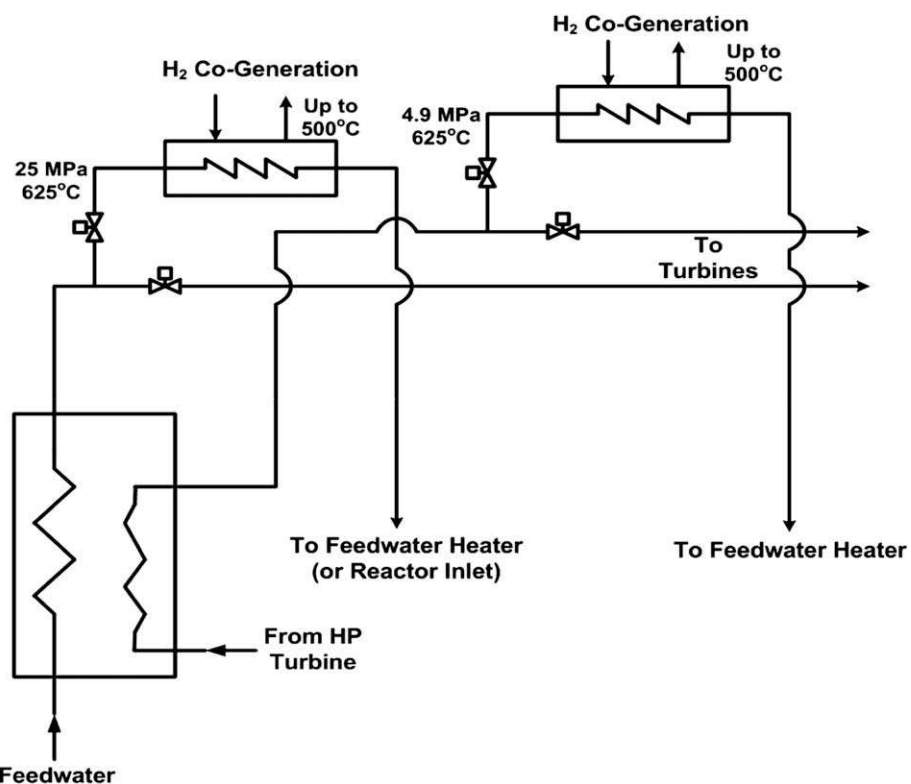


Fig. 16 – Single-reheat cycle with co-generation of hydrogen in a nuclear power plant [25].

4.1. Synergies with thermochemical hydrogen production

The emerging hydrogen economy will need an integrated group of sustainable technologies for hydrogen production, including thermochemical water splitting, high-temperature electrolysis, conventional water electrolysis and other hybrid methods (combining thermochemical and electrolytic processes). Ultimately, these technologies will complement, not compete against, one another. Electrolysis, for example, is an existing commercial technology that uses electricity to produce hydrogen from electricity. Electrolysis allows for de-centralized production of hydrogen (at perhaps a remote wind or solar power facility, or at the point of sale) and the generation of hydrogen during off-peak hours at power plants, when electricity prices and demand are lowest. From the perspective of electrical grid management, the use of hydrogen as an energy carrier is appealing, given its energy storage potential. In particular, a hydrogen economy becomes a promising possibility in the context of a diverse electricity generation system, given the significant price differences between peak and low price hours, which may or may not necessarily coincide with peak and low demand hours. Nuclear plants are most efficient when operating at rated load levels, and with technical limitations such as electrical grid transmission congestion, the use of hydrogen as an energy carrier to increase the efficiency and reliability of the electric grid becomes an attractive option. Hydrogen integrated into electrical power distribution systems could be a potential solution to the electricity storage issue, facilitating the increased use of intermittent renewable energy

sources such as wind and solar, while maintaining the necessary reliability of the electrical grid.

A certain transition period will be required to a full hydrogen economy with all light duty vehicles operating on hydrogen, specifically a period of time where infrastructure and consumption growth are considered. A practical option for this transition period is small-scale production of hydrogen using the electrolysis process together with electric power systems. During this transition, a blend of nuclear and wind energy provides emission-free and economically feasible hydrogen production. Hydrogen has been also considered as an electricity storage option, but is not yet fully competitive compared to battery storage due to its low round-trip efficiency and high investment, operation and maintenance costs.

Thermochemical cycles, by comparison, are much more efficient emerging technologies that can integrate well with electrolysis because they allow for centralized, base-load production of hydrogen and the utilization of waste heat from power plants. Thermochemical cycles have the potential to be much more efficient than electrolysis because there is no need for generation of electricity from the process heat (which experiences a significant energy loss). Effectively integrating and combining these technologies will lead to production of hydrogen at the lowest cost, with the least environmental impact.

4.2. Economic comparison with a thermochemical plant

A case study of distributed hydrogen production by electrolysis was examined by Miller et al. [37,38], for hydrogen

Table 5 – Cost comparison of different production methods for hydrogen [28]

	Off-peak electrolysis	Steam-methane reforming	Thermochemical Cu-Cl plant			
Production (tons H ₂ /day)	10 units × 1 tons/day	1 plant; 10 tons/day	1 plant; 2 tons/day	1 plant; 10 tons/day	1 plant; 50 tons/day	1 plant; 200 tons/day
Capital charge – plant (\$/GJ)	3.2	3.1	13.2	7.7	4.4	2.7
Capital charge – storage (\$/GJ)	1.0	0.8	0.5	0.5	0.5	0.5
Energy charge (\$/GJ)	12.8	8.4	6.3	6.3	6.3	6.3
Distribution charge (\$/GJ)	0	4.6	4.6	4.6	4.6	4.6
Carbon charge (\$/GJ)	0	1.6	0	0	0	0
TOTAL (\$/GJ)	17.0	18.5	24.6	19.1	15.8	14.1
Total (\$/kg)	2.41	2.67	3.49	2.71	2.24	2.00

vehicles supplied by neighbourhood fueling stations, and later extended by Naterer et al. [39] to compare electrolysis against SMR (steam-methane reforming) and thermochemical production of hydrogen with the Cu-Cl cycle. Further details of Cu-Cl plant costs were reported by Orhan et al. [40]. Cost estimates assumed a 15%/year return on investment and a 10-year amortization, which is approximately equivalent to an annual capital charge of 20%. A production cost of \$300/kW for the electrolysis cells was assumed, along with storage costs of \$800,000/ton of hydrogen via tube storage. Cost comparisons were made against this benchmark case, for centralized production of hydrogen, based on SMR and a thermochemical copper-chlorine (Cu-Cl) cycle linked with a nuclear reactor, or natural gas heating to supply the high-grade heat requirements of the thermochemical cycle.

Table 5 shows that thermochemical production becomes more competitive than electrolysis at larger capacities of hydrogen production [40]. Below capacities of between about 10 and 20 tons/day, electrolysis from off-peak electricity has a lower unit cost of hydrogen production, although the advantage reverses at higher capacities. Electrolysis costs have taken advantage of off-peak electricity, so an analogous benefit could be realized with a Cu-Cl cycle linked with SCWR. For example, a certain base-load production of hydrogen can be maintained with SCWR, but a bypass heat exchanger could re-direct steam from the power turbine to the Cu-Cl plant during off-peak periods of low electricity demand.

4.3. Hydrogen storage with combined wind and nuclear plants

The economic viability of hydrogen storage following electrolysis with a mixed wind–nuclear power plant was examined by Taljan et al. [41–43], Hajimiragha et al. [44] and Chui et al. [45], including utilization of hydrogen, oxygen and residual heat. It was shown that the system is economically feasible for high rates of return, particularly when heat and oxygen are utilized. The simulation was performed in two phases: (1) pre-dispatch phase, where optimal hydrogen charge levels are determined, and (2) a real-time dispatch on an hourly basis to maximize profits, following the hydrogen storage of the pre-dispatch phase. The evaluations were based on calculations of modified internal rates of return and net present values for a particular scenario in Ontario. The results showed that the system is more attractive for hydrogen use in

transportation and industrial markets, rather than stationary fuel cells for electricity generation. Higher and more volatile electricity prices would likely lead to better feasibility of stationary fuel cells.

5. Conclusions

This paper has presented the recent Canadian advances in nuclear-based hydrogen production, particularly involving the thermochemical Cu-Cl cycle and electrolysis. The Cu-Cl cycle was identified by Atomic Energy of Canada Limited, AECL (CRL; Chalk River Laboratories), as the most promising cycle for thermochemical hydrogen production with the Generation IV nuclear reactor, SCWR (Super-Critical Water Reactor). Recent developments of enabling technologies for the Cu-Cl cycle were presented, particularly the individual reactor designs, thermochemical properties, advanced materials, safety, reliability and linkage between nuclear and hydrogen plants. This paper has also examined the synergies of different production methods to serve both de-centralized needs with off-peak electricity (electrolysis) and centralized base-load production from a nuclear station (thermochemical methods). Specific case studies have shown that electrolysis is economically attractive at low hydrogen capacities below 10–20 tons/day, but thermochemical plants become more competitive at higher capacities.

Acknowledgements

Support of this research and assistance from Atomic Energy of Canada Limited, Ontario Research Excellence Fund, Argonne National Laboratory (International Nuclear Energy Research Initiative; U.S. Department of Energy), Natural Sciences and Engineering Research Council of Canada (NSERC), University Network of Excellence in Nuclear Engineering (UNENE) and the Canada Research Chairs (CRC) program are gratefully acknowledged.

REFERENCES

- [1] Stevens MB, Fowler MW, Elkamel A, Elhedhli S. Macro-level optimized deployment of an electrolyser-based hydrogen

- refuelling infrastructure with demand growth. *Engineering Optimization* 2008;40(10):955–67.
- [2] McQuillan BW, Brown LC, Besenbruch GE, Tolman R, Cramer T, Russ BE, et al. High efficiency generation of hydrogen fuels using solar thermochemical splitting of water. Annual Report, GA-A24972, General Atomics, San Diego, CA; 2002.
- [3] Lewis M, Taylor A. High temperature thermochemical processes, DOE hydrogen program. Annual Progress Report, Washington, DC, 2006, pp. 182–185.
- [4] Sakurai M, Nakajima H, Amir R, Onuki K, Shimizu S. Experimental study on side-reaction occurrence condition in the iodine-sulfur thermochemical hydrogen production process. *International Journal of Hydrogen Energy* 2000;23: 613–9.
- [5] Schultz K. Thermochemical production of hydrogen from solar and nuclear energy, technical report for the Stanford global climate and energy project. San Diego, CA: General Atomics; 2003.
- [6] Sadhankar RR, Li J, Li H, Ryland D, Suppiah S. Hydrogen generation using high-temperature nuclear reactors. 55th Canadian Chemical Engineering Conference, Toronto, Ontario; October 2005.
- [7] Sadhankar R. Leveraging nuclear research to support the hydrogen economy. *International Journal of Energy Research* 2007;31(12):1131–41.
- [8] Cart RH, Mazumder M, Schreider JD, Panborn JB. Thermochemical hydrogen production. Gas Research Institute for the Institute of Gas Technology, GRI Report 80-0023, vol. 1, Chicago, IL 60616; 1981.
- [9] Lewis MA, Masin JG, Vilim RB, Serban M. Development of the low temperature Cu–Cl thermochemical cycle. International Congress on Advances in Nuclear Power Plants, Seoul, Korea; May 15–19, 2005.
- [10] Serban M, Lewis MA, Basco JK, Kinetic study of the hydrogen and oxygen production reactions in the copper–chloride thermochemical cycle., AIChE 2004 Spring National Meeting, New Orleans, LA; April 25–29, 2004.
- [11] Odukoya A, Naterer GF, Electrochemical mass transfer irreversibility of cupric chloride electrolysis for hydrogen production, technical report. Faculty of Engineering and Applied Science, University of Ontario Institute of Technology, Oshawa, Ontario, Canada; 2008.
- [12] Suppiah S, Naterer GF, Lewis M, Santhanam R, Easton B, Dincer I, et al. Thermo-mechanical design of nuclear-based hydrogen production. ORF Workshops on Nuclear-based Thermochemical Hydrogen Production, Oshawa, ON (December 2007) and Chalk River, ON (October 2008).
- [13] Xiao ZF, Gammons CH, Williams-Jones AE. Experimental study of copper(I) chloride complexing in hydrothermal solutions at 40 to 300 °C and saturated water vapor pressure. *Geochimica et Cosmochimica Acta* 1998;62:2949–64.
- [14] Tsionsky M, Gun G, Glezer V, Lev O. Sol-gel derived ceramic–carbon composite electrodes – introduction and scope of applications. *Analytical Chemistry* 1994;66:1747–53.
- [15] Rabinovich L, Lev O. Sol-gel derived composite ceramic–carbon electrodes. *Electroanalysis* 2001;13:265–75.
- [16] Lev O, Wu Z, Bharathi S, Glezer V, Modestov A, Gun J, et al. Sol-gel materials in electrochemistry. *Chemistry of Materials* 1997;9:2354–75.
- [17] Anderson ML, Stroud RM, Rolison DR. Enhancing the activity of fuel-cell reactions by designing three-dimensional nanostructured architectures: catalyst-modified carbon–silica composite aerogels. *Nano Letters* 2002;3:235–40.
- [18] Naterer GF, Daggupati V, Marin G, Gabriel K, Wang Z. Thermochemical hydrogen production with a copper–chlorine cycle, II: flashing and drying of aqueous cupric chloride. *International Journal of Hydrogen Energy* 2008;33: 5451–9.
- [19] Haseli Y, Dincer I, Naterer GF. Hydrodynamic gas–solid model of cupric chloride particles reacting with superheated steam for thermochemical hydrogen production. *Chemical Engineering Science* 2008;63:4596–604.
- [20] Ferrandon MS, Lewis MA, Tatterson DF, Nankanic RV, Kumarc M, Wedgewood LE, et al. The hybrid Cu–Cl thermochemical cycle. I. Conceptual process design and H₂A cost analysis. II. Limiting the formation of CuCl during hydrolysis. NHA Annual Hydrogen Conference, Sacramento Convention Center, CA; March 30–April 3, 2008.
- [21] Naterer GF, Gabriel K, Wang Z, Daggupati V, Gravelsins R. Thermochemical hydrogen production with a copper–chlorine cycle, I: oxygen release from copper oxychloride decomposition. *International Journal of Hydrogen Energy* 2008;33:5439–50.
- [22] Wang Z, Naterer GF, Gabriel K. Multiphase reactor scale-up for Cu–Cl thermochemical hydrogen production. *International Journal of Hydrogen Energy* 2008;33:6934–46.
- [23] Chukwu C, Naterer GF, Rosen MA. Process simulation of nuclear-produced hydrogen with a Cu–Cl cycle. 29th Conference of the Canadian Nuclear Society, Toronto, Ontario; June 1–4, 2008.
- [24] Orhan M, Dincer I, Rosen MA. Thermodynamic analysis of the copper production step in a copper–chlorine cycle for hydrogen production. *Thermochimica Acta* 2008;480(1–2):22–9.
- [25] Orhan MF, Dincer I, Rosen MA. Energy and exergy assessments of the hydrogen production step of a copper–chlorine thermochemical water splitting cycle driven by nuclear-based heat. *International Journal of Hydrogen Energy* 2008;33(22):6456–66.
- [26] Orhan MF, Dincer I, Rosen MA. Thermodynamic analysis of the copper production step in a copper–chlorine cycle for hydrogen production. *Thermochimica Acta* 2008;480(1–2): 22–9.
- [27] Orhan MF, Dincer I, Rosen MA. Energy and exergy analyses of the fluidized bed of a copper–chlorine cycle for nuclear-based hydrogen production via thermochemical water decomposition. *Chemical Engineering Research and Design*, in press.
- [28] Orhan MF, Dincer I, Rosen MA. The oxygen production step of a copper–chlorine thermochemical water decomposition cycle for hydrogen production: energy and exergy analyses. *Chemical Engineering Science* 2009;64(5):860–9.
- [29] Lubis LI, Dincer I, Rosen MA. Life cycle assessment of hydrogen production using nuclear energy: an application based on thermochemical water splitting. Paper no: ES2008-54329, 8 pages, Proceedings of the ASME-International Conference on Energy Sustainability 2008, Jacksonville, Florida, USA; 10–14 August 2008.
- [30] Avsec J, Naterer GF. Thermodynamic property evaluation of copper–chlorine fluid components at high temperatures. AIAA 40th Thermophysics Conference, Seattle, WA; June 23–26, 2008.
- [31] Zhang Y, Lu L, Naterer GF. Reliability and safety assessment of a conceptual thermochemical plant for nuclear-based hydrogen generation. ASME 16th International Conference on Nuclear Engineering, Orlando, Florida; May 11–15, 2008.
- [32] Ikeda BM, Kaye MH. Thermodynamic properties in the Cu–Cl–O–H system. 7th International Conference on Nuclear and Radiochemistry, Budapest, Hungary; August 2008.
- [33] Spekkens P, Naterer GF, Gravelsins R. Ontario Power Generation, Pickering, Ontario, Canada, Personal Communication; September, 2008.
- [34] Granovskii M, Dincer I, Rosen MA, Pioro I. Thermodynamic analysis of the use of a chemical heat pump to link a supercritical water-cooled nuclear reactor and a thermochemical water-splitting cycle for hydrogen

- production. JSME Journal of Power and Energy Systems 2008; 2:756–67.
- [35] Naterer GF. Second law viability of upgrading industrial waste heat for thermochemical hydrogen production. International Journal of Hydrogen Energy 2008;33:6037–45.
- [36] Mokry S, Naidin M, Baig F, Gospodinov Y, Zirn U, Bakan K, et-al. Conceptual thermal-design options for pressure tube SCWRs with thermochemical co-generation of hydrogen, ASME Journal of Engineering for Gas Turbines and Power, in press.
- [37] Miller AJ, Duffey RB. Sustainable and economic hydrogen co-generation from nuclear energy in competitive power markets. International Energy Workshop, Laxenburg, Austria; June 24–26, 2003.
- [38] Miller AI. Electrochemical production of hydrogen by nuclear energy, Nuclear production of hydrogen – technologies and perspectives for global deployment. La Grange Park, Illinois: American Nuclear Society; 2004 [Chapter 4].
- [39] Naterer GF, Fowler M, Cotton J, Gabriel K. Synergistic roles of off-peak electrolysis and thermochemical production of hydrogen from nuclear energy in Canada. International Journal of Hydrogen Energy 2008;33:6849–57.
- [40] Orhan MF, Dincer I, Naterer GF. Cost analysis of a thermochemical Cu–Cl pilot plant for nuclear-based hydrogen production. International Journal of Hydrogen Energy 2008;33:6006–20.
- [41] Taljan G, Fowler M, Canizares C, Verbic G. Hydrogen storage for mixed wind–nuclear power plants in the context of a hydrogen economy. International Journal of Hydrogen Energy 2008;33:4463–75.
- [42] Taljan G, Fowler M, Cañizares C, Verbić G. Hydrogen storage for mixed wind–nuclear power plants in the context of a hydrogen economy. International Journal of Hydrogen Energy 2008;33(17):4463–75.
- [43] Taljan G, Cañizares C, Fowler M, Verbić G. The feasibility of hydrogen storage for mixed wind–nuclear power plants. IEEE Transactions on Power Systems 2008; 23(3):1507–18.
- [44] Hajimiragha A, Canizares C, Fowler M, Geidl M, Andersson G. Optimal energy flow of integrated energy systems with hydrogen economy considerations. iREP Symposium-Bulk Power System Dynamics and Control – VII, Revitalizing Operational Reliability, no. 4410517; 2007.
- [45] Chui F, Elkamel A, Fowler M. An integrated decision support framework for the assessment and analysis of hydrogen production pathways. Energy and Fuels 2006; 20(1):346–52.